

Effect of Pressure on Coupled Electronic Ground and Excited States Determined from Luminescence Spectra of *trans*-Dioxorhenium(V) Complexes

John K. Grey,^{†,‡} Ian S. Butler,[†] and Christian Reber^{*‡}

Contribution from the Department of Chemistry, McGill University, Montreal, Quebec H3A 2K6, Canada, and Département de Chimie, Université de Montréal, Montréal, Québec H3C 3J7, Canada

Received November 30, 2001

Abstract: Pressure-dependent luminescence spectra of *trans*-dioxo complexes of rhenium(V) with ancillary ethylenediamine ligands exhibit resolved vibronic structure in the O=Re=O symmetric stretching mode at room temperature. The intensity distribution within the vibronic progression changes with pressure, leading to band shapes that are also pressure-dependent. These spectroscopic features arise from coupled electronic states and depend on the energy differences between ground and excited states, which vary by 2500 cm⁻¹ for the three complexes with ethylenediamine, tetramethylethylenediamine, and tetraethylethylenediamine ancillary ligands. We describe the pressure-dependent vibronic structure and band shapes with anharmonic adiabatic potential energy surfaces for the ground states of all complexes. The calculated spectra reveal the pressure dependence of the energies of electronic origins, luminescence band maximums, offsets between ground- and emitting-state potential minimums, and vibrational frequencies. The largest pressure effects are observed where the coupled electronic states are close in energy.

Introduction

The application of high external pressures to molecules in order to perturb electronic structures has found much use in chemistry, physics, and materials science.^{1,2} These pressure-induced effects can be probed by electronic spectroscopy, allowing the characterization of individual electronic states. Some of the most prolific work within this area has involved pressure-tuning of the absorption and luminescence spectra of transition metal complexes.^{3,4} The effects of pressure on ligand-field parameters,^{5–9} luminescence lifetimes,³ the electronic ground state in spin-crossover compounds,¹⁰ the correlation between changes in molecular structure and electronic spectra (piezochromism),^{11,12} and the Jahn–Teller effect¹³ were inves-

tigated to obtain detailed information on the electronic structure of transition metal compounds. Despite the extensive studies in pressure-dependent electronic spectroscopy, there have been no previous comprehensive reports of the effects of pressure on coupling between ground and excited electronic states probed by luminescence spectroscopy.

Pressure-tuning spectroscopy studies aimed at interactions between excited states have been reported for doped chromium(III) systems. Reference 3 presents pressure-dependent luminescence spectra and lifetimes indicating that the spin–orbit mixing of ⁴T₂ and ²E excited states is sensitive to metal–ligand bond lengths. This excited-state interaction shows an effect of pressure on both structural and electronic properties of the emitting states. The effect of pressure on the structure of the Jahn–Teller active ⁴T₂ emitting state of a chloride lattice doped with chromium(III)¹³ is another recent example illustrating the characterization of an excited state through pressure-tuned luminescence spectroscopy with resolved vibronic structure. To investigate pressure-tuned interactions between the *ground state* and excited electronic states, we have applied high external pressures to molecular crystals of *trans*-dioxorhenium(V) complexes. From the luminescence spectra, it is possible to determine quantitatively the influence of coupling between electronic states on electronic origins, luminescence band maximums, and offsets between ground and emitting-state potential minimums. *trans*-Dioxorhenium(V) complexes have found applications in monitoring host–guest interactions by intercalating these complexes into layered materials and record-

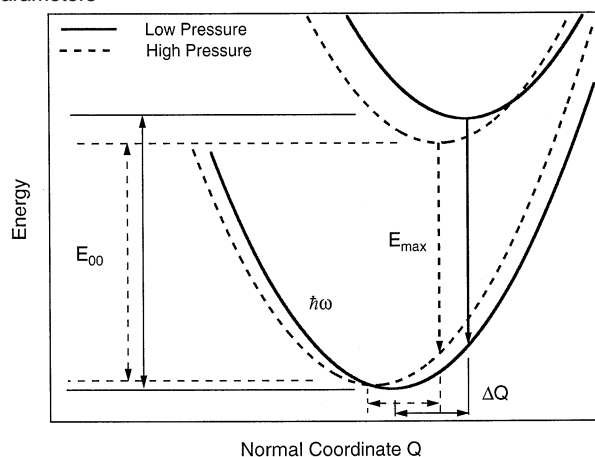
* Corresponding author. E-mail: reber@chemie.umontreal.ca.

[†] McGill University.

[‡] Université de Montréal.

- (1) Drickamer, H. G.; Frank, C. W. *Electronic Transitions and the High-Pressure Chemistry and Physics of Solids*; Chapman and Hall: New York, 1973.
- (2) Drickamer, H. G. *Acc. Chem. Res.* **1986**, *19*, 329.
- (3) Bray, K. L. *Top. Curr. Chem.* **2001**, *213*, 1.
- (4) Grey, J. K.; Butler, I. S. *Coord. Chem. Rev.* **2001**, *219–221*, 713.
- (5) Schäffer, C. E.; Lang, J. M.; Drickamer, H. G. *Inorg. Chem.* **1996**, *35*, 5072.
- (6) Parsons, R. W.; Drickamer, H. G. *J. Chem. Phys.* **1958**, *29*, 930.
- (7) Stephens, D. R.; Drickamer, H. G. *J. Chem. Phys.* **1961**, *34*, 937.
- (8) Stephens, D. R.; Drickamer, H. G. *J. Chem. Phys.* **1961**, *35*, 429.
- (9) Balchan, A. S.; Drickamer, H. G. *J. Chem. Phys.* **1961**, *35*, 356.
- (10) Gütllich, P.; Hauser, A.; Spiering, H. *Angew. Chem., Int. Ed. Engl.* **1994**, *33*, 2024.
- (11) Bray, K. L.; Drickamer, H. G. *Acc. Chem. Res.* **1990**, *23*, 55.
- (12) Bray, K. L.; Drickamer, H. G.; Schmitt, E. A.; Hendrickson, D. N. *J. Am. Chem. Soc.* **1989**, *111*, 2849.
- (13) Wenger, O. S.; Valiente, R.; Güdel, H. U. *J. Chem. Phys.* **2001**, *115*, 3819.

Scheme 1. Potential Energy Surfaces for Ground and Emitting States at Low (Solid Lines) and High (Dashed Lines) Pressures Showing the Pressure Dependence of Important Spectroscopic Parameters



ing absorption and luminescence spectra.¹⁶ Reference 16 presents various positions in which these chromophores can orient themselves within the interlamellar spaces of a host material, and the electronic spectra reveal the effect of the environment on the rhenium(V) complexes. These host–guest interactions represent a chemical pressure on the intercalated molecule whose ground-state properties are pressure-tuned. The results presented here are intended to show how pressure effects can be rationalized from models based on interacting electronic states.

Pressure decreases the volume of a solid sample and disrupts the balance between intra- and intermolecular forces. The pressure-dependent changes of the luminescence spectra reported in the following can therefore arise from both intra- and intermolecular effects. All properties, such as vibrational frequencies, vary smoothly with pressure, providing no evidence for structural phase transitions. From the pure intramolecular standpoint, pressure leads to a reduction of metal–ligand bond lengths. Electronic spectroscopy has been used to analyze such effects, often described by pressure-dependent Racah parameters, B and C , and sets of ligand-field parameters such as Dq , Ds , and Dt .^{5,14,15} The effect of external pressure on electronic transitions has been explained with pure electronic energy levels defined by these parameters. This simple approach successfully describes pressure-induced variations of unresolved band maxima but cannot rationalize vibronic band shapes, which have to be characterized with potential energy surfaces. They lead to a more detailed description of the changes the molecules experience under external pressure.^{3,13} The potential energy surfaces in Scheme 1 illustrate the effect of pressure on important observable spectroscopic quantities that define the ground and emitting states. As pressure increases, the metal–ligand bond lengths decrease and the potential minima shift to lower values of the normal coordinate, Q , in Scheme 1. The excited-state potential energy surface in Scheme 1 has its minimum at a larger value of the normal coordinate and is likely to be more strongly affected by external pressure, leading to a decrease of ΔQ , the difference of potential minima along

the normal coordinate. The energies of the two electronic states are also altered. This results in pressure-induced changes of the energy of the electronic origin, E_{00} , the band maximum, E_{\max} , the offsets between ground and emitting states, ΔQ , and the vibrational frequencies, $\hbar\omega$, observed from Raman spectra or as the spacing of a vibronic progression.

The effect of pressure on these spectroscopic quantities was studied by monitoring the luminescence of crystalline chloride salts of *trans*-[ReO₂(*N,N,N',N'*-ethylenediamine)₂]⁺, [ReO₂(*N,N,N',N'*-tetramethylethylenediamine)₂]⁺, and [ReO₂(*N,N,N',N'*-tetraethylethylenediamine)₂]⁺ complexes. These compounds will be denoted as ReO₂(en)₂Cl, ReO₂(tmen)₂Cl, and ReO₂(teen)₂Cl, respectively, throughout this report. The luminescence band maximums of the title complexes depend distinctly on the substitution of the ethylenediamine ligands and vary by $\sim 2500\text{ cm}^{-1}$ between the three complexes studied here.^{19,20} Low-temperature luminescence spectra of ReO₂(en)₂Cl and ReO₂(tmen)₂Cl complexes have been analyzed to show that the ground state is influenced by several excited states of the same symmetry through avoided crossings.¹⁹ This electronic interaction gives rise to characteristic spectra with resolved vibronic progressions involving the O=Re=O symmetric stretching mode ($\sim 900\text{ cm}^{-1}$) even at room temperature, and we present and apply a model based on potential energy surfaces as illustrated in Scheme 1 to describe quantitative changes with pressure. We use this series of closely related *trans*-dioxorhenium(V) complexes to describe how the shapes of ground-state potential energy surfaces are influenced by pressure through interactions with excited states. This effect is important for all third-row transition metal complexes due to their large spin–orbit coupling constants.

Experimental Section

The title complexes were synthesized and characterized using literature methods.^{22,23} To apply pressure to the crystalline samples, diamond-anvil cell (DAC) techniques were used. Small crystals of the title compounds, a ruby chip, and Nujol were loaded into a gasketed DAC (300- μm -diameter sample chamber, High-Pressure Diamond Optics, Tucson, AZ), and pressure was raised mechanically. The R₁ peak of the ruby emission was used to calibrate pressures,²⁴ and Nujol was the pressure-transmitting medium. Pressure-dependent luminescence and Raman spectra were collected with a Renishaw 3000 Raman microscope (20 \times and 50 \times objectives) using Spectra Physics 163-C1210 and 163-C4210 argon ion lasers (488- and 514.5-nm lines) or a Renishaw NIR 780 diode laser (782 nm) with the appropriate Renishaw notch filters as excitation sources. The pressure for experiments using the NIR diode laser was calibrated in situ by monitoring the shift of the t_{2g} phonon mode of the diamond anvils.²⁵ Since the excitation laser spot could be focused to $\sim 1\text{ }\mu\text{m}$ in diameter, we were able to minimize superposition of the intense ruby ${}^2E \rightarrow {}^4A_2$ emission on the sample spectrum by strategically placing the ruby chip in the sample hole of the gasket.

A low-temperature luminescence spectrum of crystalline ReO₂(teen)₂Cl was collected using the Renishaw 3000 Raman imaging microscope

(14) Shen, Y. R.; Bray, K. L. *Phys. Rev. B* **1997**, *56*, R473.
 (15) Ma, D.; Wang, Z.; Chen, J.; Zhang, Z. *J. Phys. C* **1988**, *21*, 3585.
 (16) Newsham, M. D.; Giannelis, E. P.; Pinnavaia, T. J.; Nocera, D. G. *J. Am. Chem. Soc.* **1988**, *110*, 3885.

(17) Winkler, J. R.; Gray, H. B. *J. Am. Chem. Soc.* **1983**, *105*, 1373.
 (18) Winkler, J. R.; Gray, H. B. *Inorg. Chem.* **1985**, *24*, 346.
 (19) Savoie, C.; Reber, C. *J. Am. Chem. Soc.* **2000**, *122*, 844.
 (20) Savoie, C.; Reber, C. *Coord. Chem. Rev.* **1998**, *171*, 387.
 (21) Savoie, C.; Reber, C.; Bélanger, S.; Beauchamp, A. L. *Inorg. Chem.* **1995**, *34*, 3851.
 (22) Lock, C. J. L.; Turner, G. *Acta Crystallogr.* **1978**, *B34*, 923.
 (23) Chatt, J.; Rowe, G. *J. Chem. Soc.* **1962**, 4019.
 (24) Piermarini, G. J.; Block, S.; Barnett, J. D.; Forman, R. A. *J. Appl. Phys.* **1975**, *46*, 2774.
 (25) Markwell, R. D.; Butler, I. S. *Can. J. Chem.* **1995**, *73*, 1019.

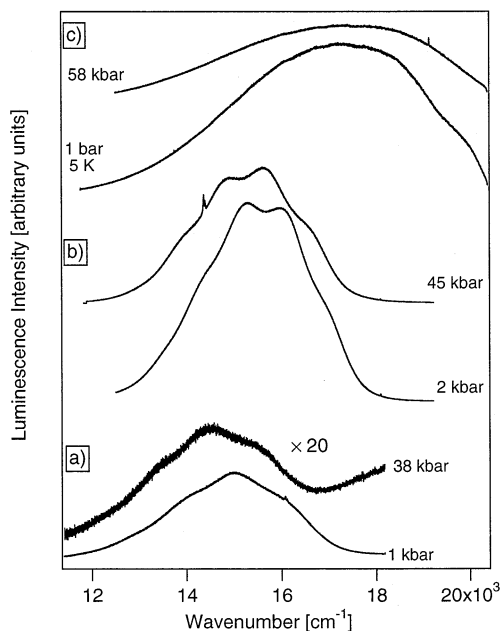


Figure 1. Low- and high-pressure luminescence spectra of (a) $\text{ReO}_2(\text{en})_2\text{Cl}$, (b) $\text{ReO}_2(\text{tmen})_2\text{Cl}$, and (c) $\text{ReO}_2(\text{teen})_2\text{Cl}$. The vibronic structure corresponds to the frequency of the $\text{O}=\text{Re}=\text{O}$ symmetric stretching mode. The ambient pressure spectrum of the $\text{ReO}_2(\text{teen})_2\text{Cl}$ complex was measured at 5 K, showing little difference from that at room temperature.

described above. Detailed low-temperature luminescence spectra for the $\text{ReO}_2(\text{en})_2\text{Cl}$ and $\text{ReO}_2(\text{tmen})_2\text{Cl}$ complexes have been reported before.¹⁹ The Raman system was configured with an elbow objective that enabled the laser spot to be focused into an Oxford Instruments CF-1204 continuous-flow helium cryostat. The luminescence spectrum of the $\text{ReO}_2(\text{teen})_2\text{Cl}$ complex dissolved in DMSO (Aldrich, ACS reagent grade) was measured at 77 K using a Linkam THMS 6000 hot/cold stage. All luminescence spectra were corrected for spectrometer response using the procedure described previously.²⁶

Luminescence lifetimes of $\text{ReO}_2(\text{teen})_2\text{Cl}$ were measured using the tripled output (355 nm) of a Continuum Mini-lite II Nd:YAG pulsed laser. The time-dependent luminescence intensities were detected with a Hamamatsu R928 photomultiplier tube and stored using a digital oscilloscope (Tektronix TDS 380) triggered by a silicon photodiode (Thorlabs FDS 100). The crystalline powder sample was cooled in the Oxford Instruments cryostat described above, and the emitted light was dispersed through a 0.5-m monochromator (Spex 500M) with a 600 lines/mm grating and filtered with a red long-pass filter (Schott RG 630). Measurements were made at ambient temperature, 100, 50, and 5 K, and decay curves were fitted with single-exponential functions to obtain the lifetimes. Absorption and diffuse reflectance spectra of $\text{ReO}_2(\text{teen})_2\text{Cl}$ were measured at room temperature with a Varian Cary 5E spectrometer.

Spectroscopic Results

Figure 1 shows luminescence spectra of all three complexes at a low and high pressure. The spectra illustrate the large variation of luminescence energies between the complexes and the effect of high pressure on the luminescence of each complex. All room-temperature spectra display a long progression involving the high-frequency $\text{O}=\text{Re}=\text{O}$ symmetric stretching mode with a frequency of $\sim 900\text{ cm}^{-1}$. The luminescence spectra of the $\text{ReO}_2(\text{tmen})_2\text{Cl}$ complex, shown as the middle traces in Figure 1, show the best resolution of vibronic progressions with well-separated members. This assignment of

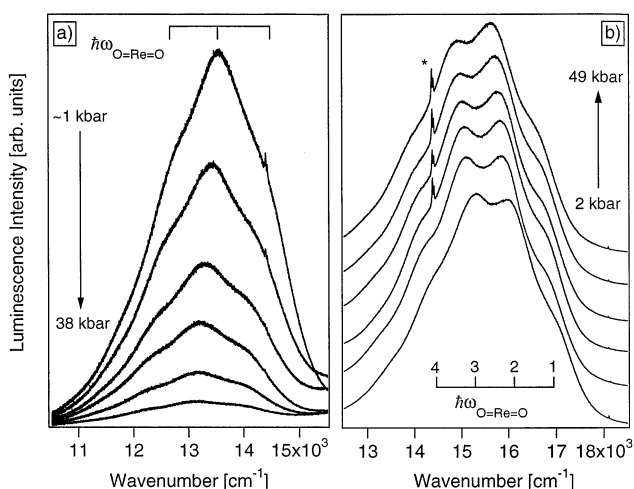


Figure 2. Examples of pressure-dependent luminescence spectra: (a) $\text{ReO}_2(\text{en})_2\text{Cl}$ from 1 to 38 kbar; (b) $\text{ReO}_2(\text{tmen})_2\text{Cl}$ from 2 to 49 kbar. The asterisk indicates the ruby luminescence used to calibrate pressure.

the vibronic progression to the $\text{O}=\text{Re}=\text{O}$ symmetric stretching mode in the luminescence is confirmed by Raman spectroscopy and well-resolved low-temperature emission spectra from the literature.^{17–21,28} Luminescence spectra of the $\text{ReO}_2(\text{teen})_2\text{Cl}$ complex do not exhibit resolved vibronic structure, even at 5 K. A shoulder does appear in the blue region of the luminescence band with an energy separation of $\sim 1400\text{ cm}^{-1}$ from the main maximum. Raman spectra of this complex show transitions at $\sim 1400\text{ cm}^{-1}$ and a strong signal for the $\text{O}=\text{Re}=\text{O}$ symmetric stretch at 1000 cm^{-1} . Luminescence lifetimes were measured across the band in order to determine whether the shoulder resolved at low-temperature was not due to an emissive impurity or different sites of the complex in our crystalline sample. The excited state lifetime at 5 K is 153 ns, compared to 152 ns at 77 K, and does not change by more than 3% across the luminescence band. The luminescence spectrum of this complex dissolved in DMSO and recorded at 77 K yields the same vibronic features as the luminescence spectrum of the crystalline complex at 5 K. These results provide evidence against multiple emitting states or luminescent impurities and allow us to include this complex in our study. Absorption and diffuse reflectance spectra of this complex at ambient temperature show that the ligand-field absorption bands and the lowest energy charge-transfer band strongly overlap. These spectroscopic results indicate that the emitting state of $\text{ReO}_2(\text{teen})_2\text{Cl}$ is different in character from the complexes with lower energy luminescence bands.

Figure 2 shows two series of pressure-dependent luminescence spectra of the $\text{ReO}_2(\text{en})_2\text{Cl}$ and $\text{ReO}_2(\text{tmen})_2\text{Cl}$ complexes. Pressure-tuning of the title complexes leads to changes in the relative intensities and energies of vibronic bands, decreases in the overall intensity of the luminescence bands, and changes in the band shapes. All pressure-induced spectroscopic changes are reversible. The magnitude of these pressure-induced changes depends strongly on the equatorial ethylenediamine ligands. Figure 2a corresponds to the least substituted complex of this series, $\text{ReO}_2(\text{en})_2\text{Cl}$. This complex exhibits the lowest energy

(27) Edwards, C. M.; Butler, I. S. *Coord. Chem. Rev.* **2000**, *199*, 1.

(28) Miskowski, V. M.; Gray, H. B.; Hopkins, M. D. In *Advances in Transition Metal Coordination Chemistry*; Che, C.-M., Yam, V. W.-W., Eds.; JAI Press: Greenwich, CT, 1996; p 159.

(26) Davis, M. J.; Reber, C. *Inorg. Chem.* **1995**, *34*, 4585.

luminescence band. The luminescence becomes very weak at pressures above ~ 40 kbar. In these spectra, we have as much as three quanta of the O=Re=O symmetric stretching mode resolved and the intensity distribution of the vibronic bands changes with pressure. The most prominent spectral feature is the rapid decrease of the overall band intensity that is likely due to more efficient nonradiative pathways at higher pressures. Figure 2b show pressure-dependent luminescence spectra of the $\text{ReO}_2(\text{tmen})_2\text{Cl}$ complex, which display the most striking changes in the relative intensity distribution within the vibronic progression. We observe up to four resolved quanta of the O=Re=O symmetric stretching mode in these spectra, and the most noticeable pressure effects are seen in the second and third members of the progression. The numbering of transitions is given below the bottom trace in Figure 2b. At low pressures, the relative intensity of the third member is higher than that of the second. As pressure increases, there is a gradual change in the intensities of the second and third peaks with the second peak becoming stronger. At pressures higher than 65 kbar, the vibronic structure is washed out and the overall intensity of the luminescence band decreases. Furthermore, as pressure increases, the luminescence onsets of the $\text{ReO}_2(\text{en})_2\text{Cl}$ and $\text{ReO}_2(\text{tmen})_2\text{Cl}$ complexes, on the high-energy side of the band, shift to lower energy. The overall luminescence band envelopes of the two complexes in Figure 2 also show a red shift that can be observed by following the vibronic peaks with increasing pressure. However, the red shift of the band maximums is not identical to that of the onsets or any individual vibronic band. This will be discussed in detail in the next section. We see that the largest change in energy of the luminescence maximums occurs with the lowest-energy emitting complex. The $\text{ReO}_2(\text{teen})_2\text{Cl}$ complex shows a small blue shift of the luminescence band maximum at higher pressures, but virtually no changes in band shape with pressure or temperature. With the pressure-dependent vibronic features laid out here, we require a model based on potential energy surfaces, as presented in Scheme 1, that correctly describes the changes in the spectroscopic quantities for each pressure.

Figure 3 depicts the pressure-dependent Raman spectra of the $\text{ReO}_2(\text{en})_2\text{Cl}$ complex in the O=Re=O symmetric stretching region. The frequency of the O=Re=O symmetric stretching mode shifts uniformly to higher wavenumber as a function of pressure ($+0.5 \text{ cm}^{-1}/\text{kbar}$), indicating an increase in the force constant of the rhenium–oxygen double bond. This trend is approximately the same for all the title complexes as illustrated by the inset in Figure 3, where we show the O=Re=O stretching frequency at various pressures for all complexes. Raman signals in the region of the Re–N(en) symmetric stretching modes show a shift to higher energy as well as a significant decrease in the area under the bands, a characteristic that is very common with the application of an external pressure.²⁷ Pressure-dependent Raman spectra of all complexes suggest that the local symmetry around the rhenium(V) center is not altered significantly, based on the smooth increases of the O=Re=O and Re–N(en) frequencies.

Discussion

Our goal is to explain all of the pressure-dependent features for the three *trans*-dioxorhenium(V) complexes. The experimental results show remarkably different luminescence proper-

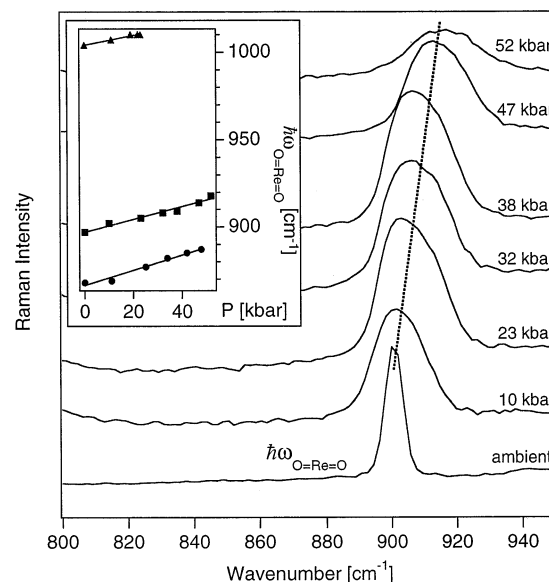


Figure 3. Ambient-temperature, pressure-dependent Raman spectra of solid $\text{ReO}_2(\text{en})_2\text{Cl}$, showing the totally symmetric O=Re=O stretching region. The inset shows examples of the pressure dependence of the O=Re=O stretching mode from all complexes studied. Squares, circles, and triangles denote $\text{ReO}_2(\text{en})_2\text{Cl}$, $\text{ReO}_2(\text{tmen})_2\text{Cl}$, and $\text{ReO}_2(\text{teen})_2\text{Cl}$, respectively.

ties for the closely related complexes, providing an ideal experimental data set that allows us to define and test theoretical models for pressure-tuning of third-row transition metal complexes. We base our model, as much as possible, on established models developed and applied to the title compounds.^{19,28}

Coupled Electronic States of *trans*- $\text{ReO}_2(\text{en})_2^+$ Complexes.

The electronic states of the title complexes have been well studied.^{18,19,28} We will only briefly discuss some of the key points to give a background necessary to understand the effects of pressure on the luminescence spectra. Idealized D_{4h} symmetry labels are used for the electronic states even though the actual overall point group symmetry is lower for the title complexes. This approximation of the local symmetry around the rhenium(V) center has been justified from the previous low-temperature absorption and emission spectroscopy on *trans*- $[\text{ReO}_2\text{L}_4]^+$ complexes.^{17–21,28} The rhenium(V) ion has the $[\text{Xe}]5d^2$ electron configuration, which becomes $(b_{2g})^2$ (corresponding to d_{xy}^2) in D_{4h} symmetry and gives rise to a nondegenerate singlet electronic ground state, $^1A_{1g}$. The lowest unoccupied orbitals are the degenerate d_{xz}, d_{yz} (e_g) levels with metal–oxo π^* character. The first excited electronic state is a doubly degenerate triplet state, 3E_g , corresponding to the $(b_{2g})^1(e_g)^1$ configuration. The energy separation of the HOMO and LUMO orbitals is described in terms of the AOM formalism by the parameter Δ_π .²⁸ Spin–orbit coupling splits the 3E_g excited state into five components, one of which has the same A_{1g} symmetry as the ground state. The luminescence originates from the lowest energy $[B_{1g}, B_{2g}]$ spin–orbit components of the 3E_g state with electron density shifting from the e_g orbitals in the first excited state to the b_{2g} orbital. The long progression in the O=Re=O stretching mode shows that the molecule distorts strongly along this normal coordinate, which suggests that the equilibrium molecular structure in the excited state is different from that of the ground state. Furthermore, there is a higher energy $^1A_{1g}$ excited state corresponding to the $(e_g)^2$ configuration as well as a A_{1g} spin–orbit component of a lower-lying $^3A_{2g}$ state arising

from this configuration.²⁸ Due to the close proximity of these two higher energy A_{1g} states and the fact that they cannot be observed spectroscopically,¹⁹ we treat them as a single effective A_{1g} state. This situation leads to three states of A_{1g} symmetry that can interact through spin-orbit coupling and configuration interaction.

An important aspect of our model for the analysis of the pressure effects shown in Figures 1 and 2 are the avoided crossings of the A_{1g} states. These electronic states are coupled, and their proximity has a large influence on the overall appearance of the emission bands. The nonzero off-diagonal matrix elements that define the coupling between states involve both the spin-orbit coupling and configuration interaction. In the literature formulation that we follow here, the configuration interaction between the lowest and highest energy A_{1g} states is given as $2^{1/2}K_{xy}$, where K_{xy} is defined in terms of the Racah parameters as $3B + C$.²⁸ The following equations give the crystal field energies of the A_{1g} states in terms of the parameters Δ_π and K_{xy} for the title complexes.²⁸ All coupling constants are set to zero for these equations.

$$E_1^{\text{CF}}[E(b_{2g})^2: A_{1g}] = 3K_{xy} \quad (1)$$

$$E_2^{\text{CF}}[E(b_{2g})^1(e_g)^1: E_g] = \Delta_\pi \quad (2)$$

$$E_3^{\text{CF}}[E(e_g)^2: A_{1g}] = 2\Delta_\pi + K_{xy} \quad (3)$$

Parameter values have been estimated from spectroscopic data^{18–20,28} and serve as the basis from which we can understand the effect of external pressure on the spectra.

Theoretical Calculation of Emission Spectra. Since we have vibrational structure resolved well enough to carry out a detailed theoretical analysis, we use the time-dependent theory of emission spectroscopy with potential energy surfaces defined by adjustable parameters to describe the electronic states of interest. This method has been covered extensively in the literature,^{29,30} and we will only briefly summarize our application of this theoretical technique.

The vertical projection of the lowest energy vibrational eigenfunction of the initial-state potential energy surface to the final state represents the first step of the emission process. This wave function is not an eigenfunction of the final potential surface and evolves with time. The time-dependent wave function, $\phi(t)$, is calculated on a one-dimensional grid representing the ground-state potential energy surface using the split-operator method by Feit and Fleck.³¹

$$\phi(t + \Delta t) = e^{(i\Delta t/4M)\nabla^2} e^{-i\Delta tV} e^{(i\Delta t/4M)\nabla^2} \phi(t) + O[(\Delta t)^3] \quad (4)$$

The vibronic luminescence spectrum is calculated as^{29,30}

$$I_{\text{lum}}(\omega) = C\omega^3 \int_{-\infty}^{+\infty} e^{i\omega t} \{ \langle \phi | \phi(t) \rangle e^{-\Gamma^2 t^2 + (iE_{00}/\hbar)t} \} dt \quad (5)$$

where ϕ is the wave function at time $t = 0$. The most important component of eq 5 is the autocorrelation function, $\langle \phi | \phi(t) \rangle$. This term describes the time-dependent overlap of the propagating wave function on the final potential energy surface. The

autocorrelation is Fourier transformed from time space to energy space to give the calculated spectrum. Γ represents a Gaussian phenomenological damping factor, which is adjusted to fit the resolution of the experimental spectrum, and E_{00} is the energy of the electronic origin. An attractive feature for the application of this method to our spectra is that potential energy functions of any form and even numerical potentials can be used as input for the states involved in the luminescence. It will be shown that the shape of the final potential energy surface is pressure-dependent, leading to the vibronic features illustrated in Figures 1 and 2.

Because luminescence spectroscopy reveals information on ground-state properties, we define a model for the ground state that describes all spectral features with theoretical and spectroscopic parameters that are intrinsic to the title systems. As a first step, we start with the simplest possible model, the harmonic oscillator approximation. The harmonic potential energy surfaces calculated for the ground states from experimental vibrational frequencies did not reproduce the actual intensity distribution of the vibronic bands. To better account for the experimental vibronic band shapes, Morse potentials were used to model the ground electronic states and were effective in reproducing the spectral features for $\text{ReO}_2(\text{tmen})_2\text{Cl}$.³² The Morse potential provides a good ad hoc description of the pressure-dependent vibronic intensity distribution in the luminescence spectra of the title complexes. However, this description does not rationalize the different luminescence characteristics of the three complexes studied here. We develop in the following a model for the ground electronic states of the title complexes that explains all pressure-induced changes in vibronic structure and vibronic band shapes using spectroscopic parameters.

Spectra Arising from Coupled Electronic States under Variable External Pressure. Previous low-temperature luminescence spectroscopic studies of the $\text{ReO}_2(\text{en})_2\text{Cl}$ and $\text{ReO}_2(\text{tmen})_2\text{Cl}$ showed that to reproduce nonreplica intensity distributions of vibronic progressions in the $\text{O}=\text{Re}=\text{O}$ and $\text{Re}-\text{N}(\text{en})$ symmetric stretching modes, a model based on interacting electronic states was needed.¹⁹ A similar model is also necessary to correctly describe the pressure-induced changes shown in Figures 1 and 2, namely, the change in the intensity distribution within the vibronic progression. Since we do not observe resolution of the $\text{Re}-\text{N}(\text{en})$ stretching modes, we limit the model to one-dimensional potential energy surfaces along the $\text{O}=\text{Re}=\text{O}$ symmetric stretching coordinate and effectively treat the title complexes as triatomic, $\text{O}=\text{Re}=\text{O}$ molecules. The potential energy surfaces of the three coupled A_{1g} states of all three *trans*-dioxorhenium(V) complexes are given by

$$V_{A_{1g}} = \begin{bmatrix} E_1 & V_{12} & V_{13} \\ V_{12} & E_2 & V_{23} \\ V_{13} & V_{23} & E_3 \end{bmatrix} \quad (6)$$

$$E_1 = E_1^{\text{CF}} + (k_{\text{Re}=\text{O}}/2)Q_{\text{Re}=\text{O}}^2 \quad (7)$$

$$E_2 = E_2^{\text{CF}} + (k_{\text{Re}=\text{O}}/2)(Q_{\text{Re}=\text{O}}^2 - 2Q_{\text{Re}=\text{O}}\Delta Q_{\text{Re}=\text{O}}) \quad (8)$$

$$E_3 = E_3^{\text{CF}} + (k_{\text{Re}=\text{O}}/2)(Q_{\text{Re}=\text{O}}^2 - 4Q_{\text{Re}=\text{O}}\Delta Q_{\text{Re}=\text{O}}) \quad (9)$$

$k_{\text{Re}=\text{O}}$ is the force constant of the $\text{O}=\text{Re}=\text{O}$ symmetric stretching mode in the ground and excited states, respectively,

(29) Heller, E. J. *Acc. Chem. Res.* **1981**, *14*, 368.

(30) Zink, J. I.; Kim Shin, K.-S. In *Advances in Photochemistry*; Volman, D. H., Hammond, G. S., Neckers, D. C., Eds.; Wiley: New York, 1991; p 119.

(31) Feit, M. D.; Fleck, J. A., Jr.; Steiger, A. *J. Comput. Phys.* **1982**, *47*, 412.

Table 1. Parameters for Potential Energy Surfaces and Time-Dependent Calculations for $\text{ReO}_2(\text{en})_2\text{Cl}$

P (kbar)	ΔQ (Å)	K_{xy} (cm^{-1})	Δ_π (cm^{-1})	$\hbar\omega_{\text{O}=\text{Re}=\text{O}}$ (cm^{-1})	V_{12} (cm^{-1})	V_{13} (cm^{-1})	V_{23} (cm^{-1})	E_{00} (cm^{-1})	Γ (cm^{-1})
1	0.110	3100	22 000	885	7250	2500	2500	14 545	285
11	0.107	3100	22 000	885	7215	2500	2500	14 421	290
23	0.106	3100	22 000	885	7215	2500	2500	14 330	290
24	0.105	3100	22 000	890	7170	2500	2500	14 270	290
28	0.105	3100	22 000	890	7150	2500	2500	14 204	295
30	0.103	3100	22 000	890	7135	2500	2500	14 172	295
33	0.103	3100	22 000	895	7115	2500	2500	14 147	295
38	0.102	3100	22 000	895	7105	2500	2500	14 127	295
38	0.100	3100	22 000	895	7080	2500	2500	14 097	300

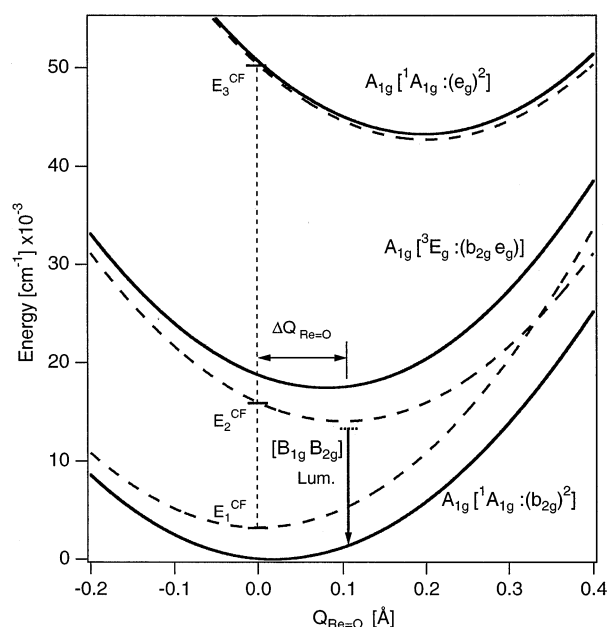


Figure 4. Coupled potential energy surfaces calculated from eq 6. Solid and dashed lines represent adiabatic and diabatic potentials, respectively. The lowest adiabatic surface corresponds to the electronic ground state used to calculate luminescence spectra. The crystal field energies E_i^{CF} (eqs 1–3) for all three A_{1g} states are given along the vertical dashed line at $Q = 0$.

where $k = 4\pi^2 M(\hbar\omega)^2$; M is the mass of the mode (16 g/mol) and $\hbar\omega$ is the frequency of the $\text{O}=\text{Re}=\text{O}$ stretching mode determined from Raman spectroscopy (in cm^{-1}) given in Table 1. $\Delta Q_{\text{Re}=\text{O}}$ is the offset of the potential energy minimums of the A_{1g} state arising from the $(b_{2g})^1(e_g)^1$ configuration along the normal coordinate. We use $2 \Delta Q_{\text{Re}=\text{O}}$ for the offset of the highest energy A_{1g} state, which arises from the $(e_g)^2$ configuration. The diabatic surfaces, E_1 , E_2 , and E_3 , represent three harmonic potential energy surfaces for A_{1g} states offset along the energy ordinate by the crystal field energies for each state and coupled through the off-diagonal elements, V_{12} , V_{13} , and V_{23} , as illustrated in Figure 4. We obtain the lowest energy adiabatic potential energy of the ground state as the first eigenvalue of the 3×3 matrix in eq 6. This anharmonic ground-

state potential surface is shown in Figure 4 and used to calculate pressure-dependent luminescence spectra.

This model of three interacting states has three avoided crossings. Figure 4 only shows the lowest energy crossing; the others are off the figure at higher energy. We find that the lowest energy crossing is the most important due to the close proximity of the lower energy A_{1g} states, but neglecting the other two crossings leads to unsatisfactory calculated spectra. With the displacement of potential surfaces along the normal coordinate and the energy offset, the surface of the ground state is flattened for $Q_{\text{Re}=\text{O}} > 0$. The emitting state in this model is approximated as a harmonic potential energy surface that represents the lowest energy spin–orbit component of the 3E_g excited state. Luminescence occurs from the lowest, most harmonic vibrational level of this state. We neglect the decrease of the force constant of the $\text{O}=\text{Re}=\text{O}$ symmetric stretching mode in the excited state and set this value equal to the force constant of the ground state, $k_{\text{Re}=\text{O}}$. This approximation is sufficient for the resolution of the spectra in Figures 1 and 2.

We calculate spectra based on the model with three A_{1g} coupled states using eqs 6–9. K_{xy} and Δ_π values for the $\text{ReO}_2(\text{en})_2\text{Cl}$ and $\text{ReO}_2(\text{tmen})_2\text{Cl}$ complexes are taken from previous low-temperature work.¹⁹ We keep the K_{xy} and Δ_π parameters independent of pressure and vary only one coupling constant to replicate the experimental spectra. This choice is justified by the small variation of the energies of the luminescence maximums in Figures 1 and 2. It is on the order of 300 cm^{-1} between ambient pressure and 40 kbar and corresponds to $\sim 2\%$ of the luminescence energy. Such a small variation of K_{xy} and Δ_π is well within the error of these parameters, which we estimate to be on the order of 5%. The value of the parameter Δ_π is the same for all three *trans*-dioxorhenium(V) complexes. Preliminary density functional theory (DFT) calculations show that the energy separation on the HOMO–LUMO gap, Δ_π , does not vary significantly between the three complexes studied.³³ The K_{xy} parameter varies by $\sim 1000 \text{ cm}^{-1}$ between the title complexes, and this variation is the main reason for the variation of the luminescence energies in Figure 1. The coupling between the two lowest energy A_{1g} states, V_{12} , is varied to describe the pressure-dependent shape of the ground-state potential surface. The other two coupling constants, V_{13} and V_{23} , are then set to equal values on the order of matrix elements coupling these states and are pressure independent. The pressure dependence of the coupling constant V_{12} is likely to reflect both intra- and intermolecular effects, and we see that variation of this parameter best reproduces the flattening of the ground-state adiabatic

(32) (a) Grey, J. K.; Triest, M.; Butler, I. S.; Reber, C. J. *Phys. Chem. A* **2001**, *105*, 6269. (b) The Morse potential energy surface of the ground electronic state describes emission band anharmonicity phenomenologically. The Morse potential adjustable parameter, D , was lowered to increase anharmonicity, such as for the lower energy emitting complexes, and raised to reproduce the effect of pressure on experimental band shapes. The Morse potential that we employed for the ground electronic state in our initial work was: $E_{\text{GS}} = D(1 - e^{-(0.1218\hbar\omega/(Dm)^{1/2}Q)})^2$, $\hbar\omega$ is the vibrational energy of the displaced normal coordinate (in cm^{-1}), m is the mass of the vibrational mode (in g/mol), D is the dissociation energy (in cm^{-1}), and Q is the normal coordinate (in Å).

(33) (a) Grey, J. K.; Butler, I. S.; Reber, C., unpublished results. (b) Landry-Hum, J.; Tessier, V.; Ernzerhof, M.; Reber, C. *Coord. Chem. Rev.*, in press.

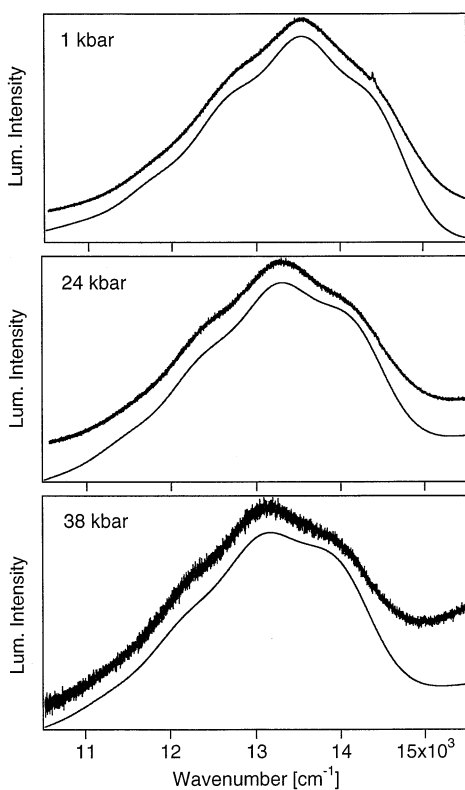


Figure 5. Examples of experimental pressure-dependent luminescence spectra compared to calculations obtained from the coupled potential energy surfaces for $\text{ReO}_2(\text{en})_2\text{Cl}$ with the parameter values in Table 1. Top and bottom traces in each panel denote experimental and calculated spectra, respectively. Spectra are offset along the ordinate for clarity.

surface and yields a better fit to experimental spectra on the “red” side of the luminescence band.

The offset, $\Delta Q_{\text{Re=O}}$, of the coupled potential energy surfaces along the $\text{O}=\text{Re}=\text{O}$ stretching coordinate is adjusted to reproduce the pressure-induced changes in vibronic structure. This parameter shows a strong pressure dependence, which could again arise from both intra- and intermolecular effects, but it is the molecular electronic structure that leads to the distinct differences between the pressure dependence of the luminescence spectra of the three complexes. For each calculation, we consider the first resolved, highest energy, member of the vibronic progression as the origin of the emission and use it to define E_{00} , the energy of electronic origin of the calculated spectra in eq 5. We set the frequency of the $\text{O}=\text{Re}=\text{O}$ stretching mode, $\hbar\omega$, in the calculated spectra to the value from the pressure-dependent Raman spectra. Figures 5–7 compare calculated and experimental pressure-dependent luminescence spectra of the title complexes and Tables 1–3 contain all parameter values used. For $\text{ReO}_2(\text{en})_2\text{Cl}$ and $\text{ReO}_2(\text{tmen})_2\text{Cl}$, the agreement between experimental and calculated spectra is excellent and allows us to discuss the quantitative variation of $\Delta Q_{\text{Re=O}}$, E_{00} , and the energy of the band maximums in the following. The Supporting Information contains all calculated spectra for these complexes.

The calculated spectra in best agreement with the experiment were obtained for $\text{ReO}_2(\text{tmen})_2\text{Cl}$. This compound shows the relatively intense luminescence in Figures 2 and 6 making a baseline correction unnecessary, and its well-resolved vibronic transition allows for an easy adjustment of the parameters in Table 2. The calculated spectra of $\text{ReO}_2(\text{en})_2\text{Cl}$ were adjusted

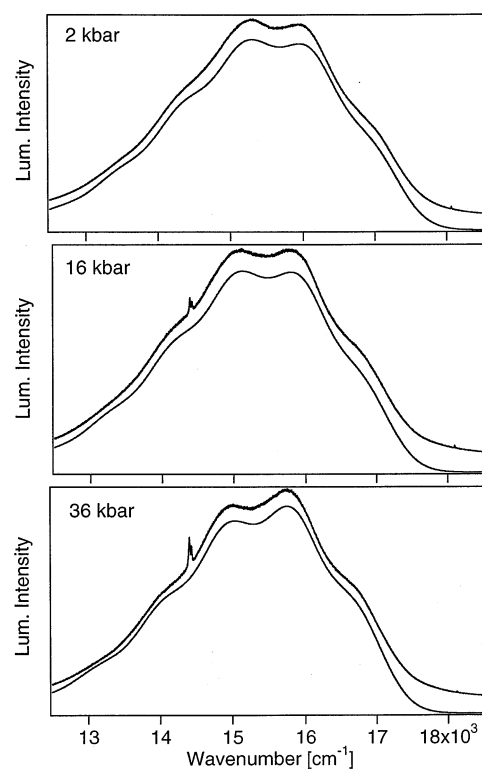


Figure 6. Examples of experimental pressure-dependent luminescence spectra compared to calculations obtained from the coupled potential energy surfaces for $\text{ReO}_2(\text{tmen})_2\text{Cl}$ with the parameter values from Table 2. Experimental spectra are offset along the ordinate for clarity.

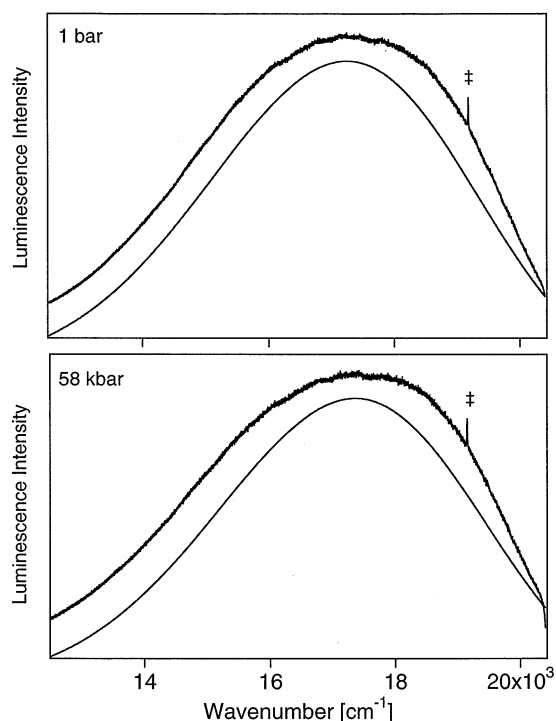


Figure 7. Pressure-dependent luminescence spectra of $\text{ReO}_2(\text{teen})_2\text{Cl}$ compared to calculations obtained with the parameter values in Table 3. Experimental spectra are offset along the ordinate for clarity. The ‡ symbols denote the Raman active t_{2g} phonon mode of the diamond anvils.

to compensate for the baseline by adding a linear function to the calculated spectrum. This baseline becomes important for the weak luminescence bands at high pressure. At higher

Table 2. Parameters for Potential Energy Surfaces and Time-Dependent Calculations for $\text{ReO}_2(\text{tmen})_2\text{Cl}$

P (kbar)	ΔQ (Å)	K_{xy} (cm^{-1})	Δ_r (cm^{-1})	$\hbar\omega_{\text{O}=\text{Re}=\text{O}}$ (cm^{-1})	V_{12} (cm^{-1})	V_{13} (cm^{-1})	V_{23} (cm^{-1})	E_{00} (cm^{-1})	Γ (cm^{-1})
2	0.120	2000	22 000	880	5850	2500	2500	17 098	285
16	0.118	2000	22 000	885	5840	2500	2500	16 934	285
20	0.116	2000	22 000	890	5830	2500	2500	16 927	280
30	0.115	2000	22 000	890	5815	2500	2500	16 878	280
36	0.113	2000	22 000	895	5805	2500	2500	16 821	280
45	0.112	2000	22 000	895	5800	2500	2500	16 728	280
49	0.111	2000	22 000	900	5790	2500	2500	16 671	280
52	0.110	2000	22 000	900	5780	2500	2500	16 645	285
58	0.110	2000	22 000	900	5770	2500	2500	16 630	300

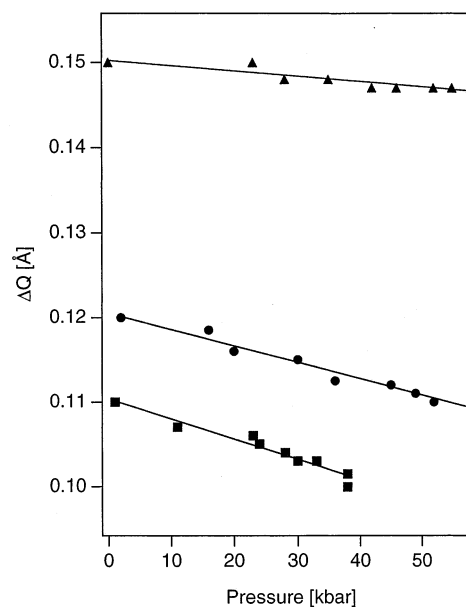
Table 3. Parameters for Potential Energy Surfaces and Time-Dependent Calculations for $\text{ReO}_2(\text{teen})_2\text{Cl}^a$

P (kbar)	ΔQ (Å)	K_{xy} (cm^{-1})	Δ_r (cm^{-1})	$\hbar\omega_{\text{O}=\text{Re}=\text{O}}$ (cm^{-1})	V_{12}^a (cm^{-1})	E_{00} (cm^{-1})	Γ (cm^{-1})
0.001	0.150	400	22 000	1000	3500	21 077	600
23	0.150	400	22 000	1000	3500	21 077	600
28	0.148	400	22 000	1000	3500	21 077	600
35	0.148	400	22 000	1000	3500	21 077	600
42	0.148	400	22 000	1000	3500	21 077	600
46	0.147	400	22 000	1000	3500	21 077	600
52	0.147	400	22 000	1000	3500	21 077	600
55	0.147	400	22 000	1000	3500	21 077	600
58	0.147	400	22 000	1000	3500	21 077	600

^a Coupling between the highest energy A_{1g} state and the lower energy A_{1g} states is neglected in calculating spectra for the $\text{ReO}_2(\text{teen})_2\text{Cl}$ complex ($V_{13} = V_{23} = 0$).

pressures, the signal-to-noise ratio decreases as well, which made fitting the high-pressure spectra difficult. Despite this problem, the intensity ratio of the first and second peaks is clearly seen to change with pressure in Figures 2 and 5, leading to reliable calculated spectra. The luminescence characteristics of the $\text{ReO}_2(\text{teen})_2\text{Cl}$ complex shown in Figures 2 and 7 are markedly different from the other two complexes, forcing us to use a simplified version of the model described above. Coupling from the highest energy A_{1g} state to the others is neglected because of the large energy separation between A_{1g} states leading to a ground-state potential surface that is almost harmonic. The calculated spectra are very similar to those obtained for a harmonic ground-state potential. Moreover, the luminescence spectrum of this complex was only weakly affected by pressure, and the effective coupling between two A_{1g} states was held constant for all pressures. The lack of resolved vibronic structure in the luminescence of $\text{ReO}_2(\text{teen})_2\text{Cl}$ leads to a situation with less constraints on model parameter values. We use the frequency of the $\text{O}=\text{Re}=\text{O}$ symmetric stretching mode from the pressure-dependent Raman spectra. The energy of the electronic origin, E_{00} , was estimated and kept independent of pressure. A value for K_{xy} was chosen for this complex based on the established trend that interelectronic repulsion decreases for increased substitution on ethylenediamine ligands.^{38,39} The offset $\Delta Q_{\text{Re}=\text{O}}$ was then adjusted to lead to an acceptable agreement between experiment and calculated spectra.

We found that a model with only one avoided crossing and two coupled states is not sufficient to reproduce all experimental

**Figure 8.** ΔQ versus pressure for $\text{ReO}_2(\text{en})_2\text{Cl}$ (squares), $\text{ReO}_2(\text{tmen})_2\text{Cl}$ (circles), and $\text{ReO}_2(\text{teen})_2\text{Cl}$ (triangles) obtained from the potential energy surfaces used to calculate spectra.

luminescence bands. Some examples of these fits are also included in Supporting Information. Traditional theoretical models^{34–37} for pressure-dependent electronic spectra involve analytical pressure-dependent terms that are added to the potential energy surfaces. We were not able to successfully apply these models to fit our spectra.

The most important results of the calculations shown in Figures 5–7 and Tables 1–3 are the quantitative pressure effects on the spectroscopic parameters of the *trans*-dioxorhenium(V) complexes. The trend for normal coordinate offsets, $\Delta Q_{\text{Re}=\text{O}}$ in eqs 7–9, at ambient pressure shows that as the ethylenediamine ligand becomes more substituted, the distortion along the $\text{O}=\text{Re}=\text{O}$ stretching mode becomes larger. $\Delta Q_{\text{Re}=\text{O}}$ is adjusted to reproduce the changes in vibronic structure, and Figure 8 shows its pressure dependences for all three complexes. We observe that this parameter decreases uniformly with pressure, which is expected as the rhenium–oxygen double bond lengths decrease with pressure. $\Delta Q_{\text{Re}=\text{O}}$ varies the most with pressure for $\text{ReO}_2(\text{en})_2\text{Cl}$ at -3×10^{-4} Å/kbar, followed by $\text{ReO}_2(\text{tmen})_2\text{Cl}$ at -2×10^{-4} Å/kbar, and, last, $\text{ReO}_2(\text{teen})_2\text{Cl}$, which shows little change at -5×10^{-5} Å/kbar. These values illustrate how pressure changes metal–oxo bond distances with similar ancillary ligands by following the pressure-induced changes in the vibronic structure.

An experimental feature that is often reported in pressure-tuning spectroscopic studies is the shift of the band maximum

(34) Lin, S. H. *J. Chem. Phys.* **1973**, *59*, 4458.(35) Tompkins, R. C. *J. Chem. Phys.* **1978**, *69*, 579.(36) Tompkins, R. C. *J. Chem. Phys.* **1980**, *72*, 3449.(37) Kesarwani, R. N.; Varshni, Y. P. *J. Chem. Phys.* **1984**, *81*, 5508.(38) Lever, A. B. P.; London, G.; McCarthy, P. J. *Can. J. Chem.* **1977**, *55*, 3172.(39) Lever, A. B. P.; Walker, I. M.; McCarthy, P. J.; Mertes, K. B.; Jircitano, A.; Sheldon, R. *Inorg. Chem.* **1983**, *22*, 2252.

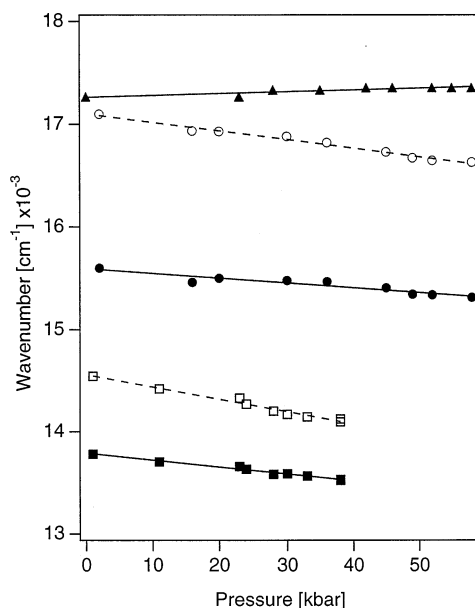


Figure 9. Emission energy maximum, E_{\max} , (solid symbols) and energy of electronic origin, E_{00} , (open symbols) versus pressure, for $\text{ReO}_2(\text{en})_2\text{Cl}$ (squares), $\text{ReO}_2(\text{tmen})_2\text{Cl}$ (circles), and $\text{ReO}_2(\text{teen})_2\text{Cl}$ (triangles).

with pressure. This particular observation can be explained most easily in terms of pure electronic energy diagrams for a molecule held frozen at its ground-state equilibrium geometry. Band maximums are not directly obtained for the spectra in Figures 1 and 2 because of the resolved vibronic structure. We determine this value by using the parameters in Tables 1–3 and increasing the phenomenological damping factor, Γ , until an unresolved calculated spectrum is obtained, for which the maximum is easily determined. The luminescence bands of $\text{ReO}_2(\text{en})_2\text{Cl}$ and $\text{ReO}_2(\text{tmen})_2\text{Cl}$ shift to lower energy by -8 and $-6 \text{ cm}^{-1}/\text{kbar}$, respectively. The $\text{ReO}_2(\text{teen})_2\text{Cl}$ complex shows a slight blue-shift of $+2 \text{ cm}^{-1}/\text{kbar}$ with increasing pressure. Figure 9 shows the pressure dependence of the band maximum, E_{\max} , and the calculated value of the electronic origin, E_{00} .

The behavior of the calculated E_{\max} and E_{00} values with pressure shows how the luminescence band maximums and onsets depend on the displacement of the emitting-state potential surface relative to the ground-state potential surface both in energy and in normal coordinate offset. We observe that these quantities do not have the same pressure dependence. The E_{00} values for both $\text{ReO}_2(\text{en})_2\text{Cl}$ and $\text{ReO}_2(\text{tmen})_2\text{Cl}$ decrease faster than the band maximums with pressure. This difference illustrates that the energy of the band maximums is influenced not only by the electronic energies but also by the pressure-dependent displacement, $\Delta Q_{\text{Re}=\text{O}}$, of the potential minimums along the normal coordinate. Since luminescence of $\text{ReO}_2(\text{teen})_2\text{Cl}$ lacks well-resolved vibronic structure and shows only small shifts in band energies, the change in normal coordinate offset is sufficient to reproduce shifts in band maximums. This is accomplished by holding the E_{00} value of the emitting state constant and adjusting $\Delta Q_{\text{Re}=\text{O}}$, based on the range of frequency shift of this mode in the pressure-dependent Raman spectra, to replicate the energy shift of the band. The limits of the approach based on pure electronic levels are quantitatively illustrated here since these models cannot predict the different behavior of E_{\max} and E_{00} with pressure.

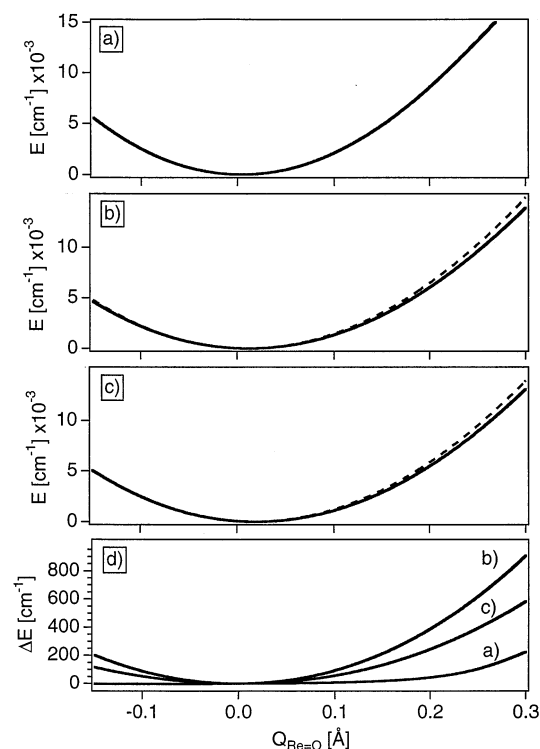


Figure 10. Ground-state adiabatic potential energy surfaces at the lowest (solid) and highest (dashed) pressures. (a) $\text{ReO}_2(\text{en})_2\text{Cl}$, 1 (solid line) and 38 kbar (dashed line); (b) $\text{ReO}_2(\text{tmen})_2\text{Cl}$, 2 (solid line) and 58 kbar (dashed line); and (c) $\text{ReO}_2(\text{teen})_2\text{Cl}$, ambient (solid line) and 57 kbar (dashed line). The bottom panel, (d), shows the difference between the adiabatic ground-state potential energy surfaces at the lowest and highest pressure for each complex.

The ground-state potential energy surfaces show distinct changes that can be correlated with the proximity of avoided crossings. The overall qualitative trend found in all experimental luminescence spectra is that pressure “pushes up” the ground-state adiabatic potential at large values of Q so that it becomes more harmonic in character. Both intra- and intermolecular effects are likely responsible for this behavior. Panels a–c in Figure 10 illustrate the effect of pressure-dependent coupling on the ground-state potential energy surfaces for all three *trans*-dioxo complexes at the lowest and highest pressure for which we obtained data. The difference between the lowest and highest pressure potential energy surfaces for the three complexes is shown in Figure 10d. These traces give the quantitative variations of the ground-state potential as a function of pressure over a significant range of $Q_{\text{Re}=\text{O}}$, information that can only be obtained through luminescence spectroscopy. The pressure-induced changes to the shape of the ground-state potential energy surface and the calculated spectra are most pronounced for the lower energy emitting complexes, because they have avoided crossings at low energies, as illustrated in Figure 4.

Our analysis shows that the ground-state potential energy surface is significantly altered by pressure as shown in Figure 10. It is interesting to note that the pressure-induced increase in vibrational frequency, illustrated in Figure 3, is not sufficient to explain the change of the potential energy surfaces in Figure 10. This change in the $\text{O}=\text{Re}=\text{O}$ stretching frequency involves a small region of the ground-state potential energy surface near its minimum and far from the Franck–Condon region where the luminescence occurs, but the Raman results are important

to define the effect of pressure on the vibrational frequency used in our calculations. The vibronic luminescence spectra provide insight into a much larger part of the ground-state potential energy surface than the fundamental vibrational transition probed by Raman spectroscopy, and the combination of electronic and vibrational spectroscopy under external pressure allows the identification of pressure-induced variations of all parameters, as illustrated in Scheme 1 and Tables 1–3.

Conclusion

Luminescence spectra of *trans*-dioxo complexes of rhenium(V) and a model based on coupled electronic states allow us to reproduce all of the pressure-dependent vibronic features observed in the luminescence bands and to compare quantitative pressure effects for a series of related complexes. The analysis provides new insight into the effect of pressure on interactions between electronic states. With resolved vibronic spectra, it is

feasible to determine the pressure dependence of molecular quantities. We observe that pressure-induced changes of the ground-state potential energy surfaces depend on interactions with excited electronic states.

Acknowledgment. This work was made possible by grants from the Natural Sciences and Engineering Research Council (Canada).

Supporting Information Available: Comparison of all experimental and calculated luminescence spectra for the $\text{ReO}_2(\text{en})_2\text{Cl}$ and $\text{ReO}_2(\text{tmen})_2\text{Cl}$ complexes used to compile Table 1 and Figures 8 and 9, alternative calculated spectra showing that a model based on only two coupled states is not adequate (PDF). This material is available free of charge via the Internet at <http://pubs.acs.org>.

JA012629N